https://doi.org/10.1016/j.solmat.2021.110983

Revised Ms. SOLMAT-S-20-02273

Formulation of highly stable PCM nano-emulsions with reduced supercooling for thermal energy storage using surfactant mixtures

Liu Liu[a], Jianlei Niu[b], Jian-Yong Wu[a, *]

[a] *Department of Applied Biology & Chemical Technology, The Hong Kong Polytechnic University, Hung Hom, Kowloon, Hong Kong*

[b] *Department of Building Services Engineering, The Hong Kong Polytechnic University, Hung Hom, Kowloon, Hong Kong*

ABSTRACT

This study was to develop stable phase change material (PCM)-water nano-emulsions with low supercooling and low viscosity using two-surfactant mixtures by the phase inversion temperature (PIT) method. The PCM agent n-hexadecane was mixed with Brij L4 as the primary surfactant and polyethylene-block-poly(ethylene glycol) (PE-*b*-PEG), Tween 60 or Tween 80 as a co-surfactant to form stable nano-emulsions. The results showed that the droplet size, viscosity and PIT point as well as the stability of PCM nano-emulsions were strongly dependent on the combination, mass ratio and total concentration of the two surfactants. In 25% (w/w) PCM nano-emulsions, an optimum formulation was the surfactant combination of Brij L4 and Tween 60 at 6:4 mass ratio, mixed with PCM at 11:20 mass ratio. The corresponding nano-emulsion had a high stability, a small droplet size of 60 nm and desirable Newtonian fluid behaviour with a relatively low viscosity of 50 mPa·s. The addition of n-octacosane as a nucleating agent was effective to reduce the emulsion supercooling, though the supercooling degree was notably increased after multiple thermal cycles. The optimized 25% PCM nano-emulsion with 2% (w/w) n-octadecane showed an excellent stability over 120 days and 300 thermal cycles with a droplet size below 80 nm, a supercooling degree of ~5 °C and a latent heat of ~50 J/g, which was very promising for further development and application as a cooling storage medium.

Keywords: PCM nano-emulsion; Phase inversion temperature; Surfactant mixtures; Stability; Supercooling; Viscosity.

* Corresponding author.
E-mail address: Jian-yong.wu@polyu.edu.hk (J.Y. Wu).

1. Introduction

Thermal energy storage (TES) is one of the most important and efficient means for utilization of excessive energy. Although TES technologies may be applied to store sensible, latent and thermochemical heat [1-3], latent heat storage using phase change materials (PCMs) is the most favourable as PCMs can absorb and release a large amount of heat at nearly a constant temperature [4-6]. Particularly, considerable research effort has been devoted to the development of PCM-based heat transfer fluids (HTFs) for storage of latent heat [7-10]. There are three main types of latent functionally thermal fluids including clathrate hydrate slurries, microencapsulated PCM (MPCM) slurries, and PCM emulsions [11]. PCM emulsions are formed by dispersing PCM as fine droplets into an immiscible carrier liquid with the assistance of surfactants. Compared to MPCM slurries, PCM emulsions have the advantages of low cost, simple fabrication, low viscosity and good operation stability. In addition, heat transfer is enhanced due to the large surface-to-volume ratio and negligible thermal resistance of a thin protective surfactant layer between the PCM and the carrier liquid [12, 13].

However, the poor stability and high degree of supercooling are two main challenges for the development and application of PCM emulsions for TES systems. PCM emulsions are thermodynamically unstable owning to their high surface free energy. Reduction of the droplet size to the nanoscale (< 200 nm) or the formation of PCM nano-emulsions is regarded as one of the most effective methods for improving the emulsion stability. Schalbart et al. [14] attained a tetradecane nano-emulsion with droplet size around 200 nm, which remained stable over six months. By D-phase method, Chen et al. [15] fabricated n-hexadecane and n-octadecane nano-emulsions which were stable over 210 days. In the previous studies from our group [16, 17], stable n-hexadecane nano-emulsions with droplet size below 100 nm have been attained by low-energy emulsification method, including phase inversion temperature (PIT) and emulsion inversion point (EIP) method.

Supercooling is the process of cooling a liquid to a temperature below its melting or freezing temperature without crystallization [6, 18]. Supercooling is severe in PCM nano-emulsions due to the dominance of homogeneous nucleation, which is common in a pure liquid with the nucleation rate being a function of the bulk volume [19]. PCM nucleation takes place in the nano-droplets individually. Because of the very small volume, the probability for the formation of nucleation sites is very low so that a much lower temperature is required for crystal formation. The addition of various nucleating agents such as nanoparticles and alkanes, and their derivatives with higher melting temperatures is the most common approach to reducing

supercooling, which is to shift homogeneous nucleation to heterogeneous nucleation [20, 21]. Wang et al. [22] used 2 wt% graphite nanoparticles in OP10E emulsions with droplet size 3-4 μm, leading to a complete elimination of supercooling. Xiang et al. [23] prepared a paraffin emulsion (particle size distribution between 0.2 to 1.5 μm) added with 1.2 wt% graphene and achieved a low supercooling degree of 0.27 ℃.

Hydrophobic nano-SiO_2 has been used as a nucleating agent in a previous study in n-hexadecane emulsions, achieving a low supercooling degree of 0.8 ℃ at 0.5 wt% content [17]. However, high-energy emulsification methods are usually needed to disperse the nanoparticles into PCM droplets which have relatively large droplet sizes in the microscale instead of nanoscale. Our group has previously attempted to disperse the same hydrophobic nano SiO_2 into the n-hexadecane nano-droplets (< 100 nm) by the EIP method [16], though the supercooling was not effectively controlled due mainly to the low encapsulation efficiency within the PCM nano-droplets. Moreover, the nano-SiO_2 dispersed in PCM is prone to aggregation and precipitation, causing instability of the nano-emulsions. Although the instability issue is less severe with alkanes and their derivatives because of good compatibility, they are also less effective for supercooling reduction. Cabaleiro et al. [9] prepared n-heptadecane and commercial paraffin RT21HC nano-emulsions, with one alkane and two commercial paraffin waxes as additives, but had rather large supercooling up to 10.5 ℃.

The supercooling of PCM emulsions can also be influenced by surfactants. Sakai et al. [24] reported that surfactants with longer hydrocarbon chains effectively facilitated the nucleation in n-hexadecane emulsions. As reported previously [25, 26], surfactants with similar hydrocarbon chains (16 or 18 carbons) could mitigate the supercooling of n-hexadecane emulsions. Several polyvinyl alcohols with different hydrocarbon chains could lower the supercooling degree of n-octadecane emulsions to 2 ℃ [27]. On the other hand, the use of mixed surfactants may be more effective to lower the interfacial tension than single ones [28], increasing the emulsion stability against multiple destabilization processes [29, 30].

Based on the above background as well as our previous studies, this work aimed to formulate highly stable, low-supercooling and low-viscosity n-hexadecane nano-emulsions through the use of two surfactant mixtures and the addition of nucleating agents. With these characteristics, the n-hexadecane nano-emulsions will be used as the thermal storage media that can be are easily transported through the thin pipes in a chiller for charging and in the ceiling panel for room cooling or discharging. To the best of our knowledge, such a TES system based on nano-emulsions flowing in pipes has not been reported previously. To attain the desired nano-emulsions more effectively, in the present study, we took a new approach by the

use of two mixed surfactants and assessed the key factors affecting the emulsion properties comprehensively. Specifically, the nonionic polyethoxylated (PEO) surfactant, Brij L4 was chosen as the primary surfactant because of its ability to stabilize n-hexadecane nano-emulsions by the PIT and EIP method [16]. The co-surfactant was chosen from two types of surfactants including the polymeric surfactants (PE-*b*-PEG) having longer hydrocarbon chains than, and the nonionic hydrophilic surfactants (Tween 60 and Tween 80) having the similar hydrocarbon chains to that of n-hexadecane. The PCM nano-emulsions were prepared with the PIT method and the influence of surfactant combinations and the mass ratios, and concentrations of surfactant mixture and n-hexadecane were evaluated on the properties of nano-emulsions. A pure alkane, n-octacosane, was added as a nucleating agent to further reduce the degree of supercooling without disrupting the stability of nano-emulsions.

2. Materials and methods

2.1. Materials

N-hexadecane ($C_{16}H_{34}$, 99%; C16) was purchased from International Laboratory, USA. Polyethylene glycol dodecyl ether (Brij L4, abbreviated as Brij), polymeric surfactants, polyethylene-block-poly(ethylene glycol) (PE-*b*-PEG) of number-average molecular weight M_n~1400 and ~2250 (P-1400 and P-2250, respectively) were from Sigma-Aldrich, USA. Commercial nonionic surfactants, polyethylene glycol sorbitan monooleate (Tween 80) and polyoxyethylene sorbitan monostearate (Tween 60), and sodium chloride (NaCl, 99.5%) were from Aladdin, China. N-octacosane ($C_{28}H_{58}$, 98%; C28) was purchased from TCI, Japan. All chemicals were used as received from the suppliers.

2.2. Preparation of PCM nano-emulsions

The n-hexadecane PCM nano-emulsions were formulated by the PIT method [17, 31] as illustrated in Scheme 1. Firstly, the n-hexadecane and surfactants were mixed with a magnetic stirrer at 400 rpm and the temperature was maintained above 65 ℃ according to the PIT point of samples. A higher temperature up to 75 ℃ was applied to promote the dissolution of solid PE-*b*-PEG. Distilled water was slowly added to the mixture to ensure the emulsification temperature over the PIT point and then cooled down rapidly to room temperature, yielding the PCM nano-emulsions.

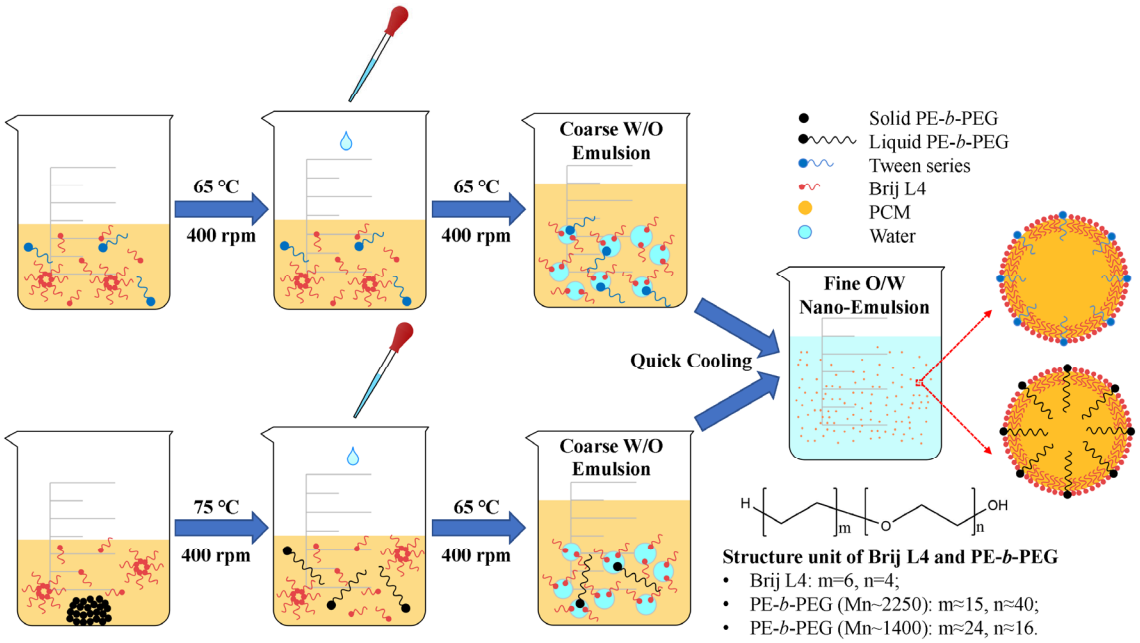

Scheme 1 Major steps for the preparation of n-hexadecane/water nano-emulsions by the PIT method. PCM oil, n-hexadecane, and surfactants were heated and mixed with a magnetic stirrer to form a homogeneous mixture and then, distilled water was slowly added to the mixture, forming coarse water-in-oil (W/O) emulsions, followed by quick cooling to room temperature, yielding the oil-in-water (O/W) nano-emulsions.

Table 1 shows the eight sets of experimental conditions including various combinations/ concentrations of the n-hexadecane and two-surfactant mixtures for preparation of the PCM nano-emulsions. Initially, the total concentration of two surfactants (Brij plus PE-*b*-PEG or Tween) was 10% and the PCM was fixed at 20% (No. 1 & 2). According to preliminary tests, the mass ratio of Brij to PE-*b*-PEG was firstly varied in the range of 7:3 to 9:1 and that of Brij to Tween was 5:5 to 9:1. Secondly, the total concentration of two surfactants was varied from 8-12%, with the PCM concentration fixed at 20% (No. 3 & 4). In the next, the PCM concentration was varied from 20-25% with the Brij and P-2250 mixture (No. 5) or 20-30% with the Brij and Tween 60 mixture (No. 6), at 20:11 mass ratio of PCM to two-surfactant mixture. Finally, n-octacosane (C28) (up to 10% of the C16 mass) was used as a nucleating agent (No. 7 & 8) since a higher C28 content (~15% of the C16 mass) could change the thermal properties of C16 [32, 33].

Table 1 Experiment variables for preparation of n-hexadecane PCM nano-emulsions (all % values in weight%).

Surfactant mixtures	Mass ratio	Surfactant content	PCM content
1. Brij + PE-*b*-PEG	7:3 to 9:1	10%	20%
2. Brij + Tween	5:5 to 9:1	10%	20%
3. Brij + P-2250	8:2	8-12%	20%
4. Brij + Tween 60	6:4	8-12%	20%
5. Brij + P-2250	8:2	11/20 of PCM mass	20-25%
6. Brij + Tween 60	6:4	11/20 of PCM mass	20-30%
7. Brij + P-2250 + 0-2% C28	8:2	11%	20%
8. Brij + Tween 60 + 0-2.5% C28	6:4	11%	25%

2.3 Determination of PIT point

The PIT point of PCM nano-emulsions was determined through measurement of the electrical conductivity [34]. Coarse emulsions containing 20% C16 and different surfactant concentrations and water (NaCl, 0.01 mol/L) were prepared by simple mixing at room temperature. The emulsions were then constantly agitated mechanically during which the electrical conductivity was measured as a function of temperature. The PIT point was corresponding to the temperature with a sharp drop in the electrical conductivity.

2.4. Analysis of droplet size

The average droplet diameter and polydispersity index (PDI) were measured by dynamic laser scatter (DLS) using a Malvern Zetasizer Nano ZS instrument which was equipped with a 4 mW He-Ne laser operating at a wave-length of 633 nm. The samples were diluted 100-fold in distilled water and measurement were carried out at 25 ℃ with a scattered angle of 173º. Triplicate measurements of 15 runs were conducted for each sample. The morphology of PCM nano-emulsions was examined with a Leica DM4000 optical microscope at 1000× magnification range. The images were processed using the Leica LAS AF software.

2.5. Viscosity

The apparent viscosity of PCM nano-emulsions was measured with a rotational viscometer using the ultra-low viscosity adapter (Brookfield, DV3T), which can measure the viscosity at a given shear rate with accuracy of ±1.0% range.

2.6. Thermal analysis

Thermal properties of the PCM nano-emulsions including melting or freezing temperature and latent heat were measured with a differential scanning calorimeter (Mettler Toledo, DSC3). The PCM nano-emulsion samples (3-5 mg) were placed in aluminium crucibles and maintained an initial temperature of 30 ℃ for 10 min. Then the samples were cooled to -5 ℃, maintained for 10 min, and finally heated to 30 ℃. The heating/cooling rate was 5 ℃/min. The thermal data were analysed and plotted using the STARe software. The onset temperature for melting and freezing was recorded, which is independent of the heating/cooling rate [35]. The difference between the onset melting and nucleation temperatures was taken as the supercooling degree of the samples.

2.7. Evaluation of the stability of the PCM nano-emulsions

The stability of PCM nano-emulsions was evaluated based on droplet size analysis and visual observation of the phase homogeneity through the long period of storage at room temperature and repeated thermal cycles [16, 17]. The procedure of one thermal cycle was slightly modified including 10 min cooling process at 0 ℃ in an ice-water bath, and 10 min heating process at 30 ℃ in a thermostatic water tank. About 5 mL of the nano-emulsion sample was filled into a glass bottle for the thermal cycle test. The formula optimization was based on the results of the sample treated after 50 thermal cycles and 15-day storage at 25 ℃. The long-term stability of the optimized samples was evaluated based the observation of appearance and analysis of droplet size and thermal properties after long period of storage at room temperature and 300 thermal cycles.

2.8. Theoretic basis for emulsion stability with surfactant mixtures and PIT method

Emulsions including nano-emulsions are thermal dynamically metastable systems, which trend to break down through several destabilization processes, e.g., gravitational separation, flocculation, coalescence, and Ostwald ripening [36, 37]. Gravitational separation including creaming and sedimentation is caused by the difference in mass density between the continuous and dispersed phase. The rate of gravitational separation can be described by Stokes' Law [38]:

$$v_{Stokes} = -\frac{2gr^2\Delta\rho}{9\eta} \tag{1}$$

where r is the droplet radius, g is the acceleration due to the gravity, $\Delta\rho$ is the density difference between the continuous and dispersed phase, η is shear viscosity of the continuous phase. This

equation indicates that smaller droplet size and density difference, or higher viscosity of the continuous phase can reduce the velocity of gravitational separation. The small size (< 90 nm) can also effectively overcome gravity due to Brownian motion [39]. The overall density of an PCM emulsion droplet ($\rho_{droplet}$) depends on the densities of PCM and the surfactant shell, as described by the following equation [40],

$$\rho_{droplet} = \frac{r\rho_{PCM} + 3\delta\rho_{shell}}{r + 3\delta} \quad (2)$$

where ρ_{PCM} and ρ_{shell} are the densities of the PCM and the surfactant within the interfacial layer, and δ is the thickness of the interfacial layer. The usage of mixed surfactants that pack more tightly creates denser interfaces, and therefore reduce the velocity of gravitational separation.

Droplet aggregation with or without film rupture is referred to as coalescence or flocculation. The dominance of the attractive forces such as van der Waals make droplets tend to flocculate or fuse together forming a larger droplet. The adsorption of mixed nonionic surfactants at the interface may increase the steric repulsion [41] and form dense interfaces that are able to improve their stability against flocculation or coalescence. On the other hand, the high levels of non-adsorbed nonionic surfactants can lead to emulsion instability owing to a depletion flocculation mechanism [29].

Ostwald ripening (OR), which is reported as the main destabilization mechanism for nano-emulsions [42], arises from the difference in Laplace pressure (Δp) between small and large droplets, which is governed by the following equation [43]:

$$\Delta p = 2\gamma\left(\frac{1}{r_1} - \frac{1}{r_2}\right) \quad (3)$$

where γ is the interfacial tension, r_1 and r_2 are radius of small and large droplets. The smaller droplets disappear and the large droplets become larger. From this equation, it is obvious that reducing the interfacial tension or difference of droplet size between r_1 and r_2 can decrease the Laplace pressure difference and hence slow down the OR rate. In addition, the OR rate (ω) can be estimated by the following equation [44],

$$\omega = \frac{dr^3}{dt} = \frac{8DC_\infty\gamma V_m}{9\rho RT} \quad (4)$$

where D is the diffusion coefficient of the dispersed molecules in the continuous phase, C_∞ is

the bulk solubility of the dispersed phase in the bulk continuous phase, V_m is the molar volume of the dispersed phase, ρ is the density of the dispersed phase, R is the gas constant, and T is the absolute temperature. The OR rate may be reduced by using mixed surfactants that can lower the interfacial tension more significantly. However, if the concentration of non-adsorbed surfactants in the continuous phase is high, the formation of surfactant micelles working as a 'bridge' promotes a net mass flow from small to large droplets.

Moreover, several factors such as storage temperature affect the emulsion stability when using the PIT method, where the temperature change induces a change in the curvature of the surfactant interfacial arrangement [45]. Typically, nonionic PEO surfactants are the most commonly used, while it is noteworthy that phase inversion does not occur for nonionic PEO surfactants having a too short or too long PEO head group and *vice versa*, a too long or too short alkyl tail [31], as illustrated by the packing parameter (p), which is equal to the ratio of the alkyl tail group to PEO head group cross-section areas [46]. At low temperatures, PEO head group is larger than the alkyl tail group ($p < 1$) due to the hydration effect; the monolayer adopting a curvature where the PEO head groups point outward, favors the formation of O/W emulsions. Conversely, the dehydrated PEO head group inducing a shrinkage of their area at a higher temperature is smaller than the alkyl tail group ($p > 1$); the monolayer adopts a curvature where the PEO head groups point inward, favoring the formation of W/O emulsions. When the cross-section areas of the PEO head group and alkyl tail group are the same ($p \approx 1$), the corresponding temperature is the PIT point, where the inversion zone has a nearby zero interfacial tension and flat curvature [30].

Immediately below the PIT point, which is often referred to as the droplet coalescence zone [47], emulsion coalescence occurs quickly. Therefore, fast crossing the PIT point from high temperature to low temperature is necessary to induce a change in the curvature of the surfactant interfacial arrangement and to produce stable O/W nano-emulsions. The storage temperature should be about 20-30 ℃ below the PIT point [47, 48]. Apart from temperature, phase inversion is facilitated by low-energy or high-energy stirring but inhibited by intermediate stirring [49]. Low-energy stirring by a magnetic stirrer tends to form large droplets and multiple emulsions during emulsification, favouring phase inversion after a quick cooling.

The above theoretical relationships suggest that the use of mixed surfactants at suitable concentrations is favourable for preparation of stable emulsions with a small droplet size, a narrow droplet size distribution or small PDI, a relatively low viscosity and a suitable PIT point. However, the mechanisms of emulsion instability are complex and dependant on multiple factors, and their interactions.

3. Results and discussion

3.1. Surfactant type on emulsion properties

3.1.1. Brij and PE-b-PEG combinations

Fig. 1 presents the photos of nano-emulsions prepared by mixtures of Brij and PE-*b*-PEG (P-2250 and P-1400) upon preparation and after 50 thermal cycles, and 15-day storage. The initial nano-emulsions with the Brij and P-2250 mixture exhibited a milky white color at 7:3 mass ratio and gradually turned to a bluish, and transparent color at 9:1 mass ration, implying the gradual decrease of droplet size. All nano-emulsions stabilized by the mixture of Brij and P-1400 displayed a similar milky white color with the droplet size in the range of 100-120 nm, irrespective of the mass ratio of Brij to P-1400. The emulsion breakdown was observed for all emulsion samples prepared with the Brij and P-1400 mixture after 15 days. The abnormal phenomenon in the last two emulsion bottles (at 8.5:1.5 and 9:1 mass ratio, after 15 days) with a top bluish layer and a bottom milky white layer was investigated by DLS and DSC analysis. It was found that the droplet size of the upper layer was about 55 nm while the latent heat was markedly lower than that of the lower layer, suggesting that sedimentation instead of creaming was responsible for the emulsion breakdown. The formation of a bottom milky layer with a higher density than water was probably attributed to the flocculation effect of polymeric surfactants. In contrast, the stability of nano-emulsions with the mixture of Brij and P-2250 was mostly much higher except for that at 7:3 mass ratio showing creaming after 15 days. Overall, the combination of Brij and PE-*b*-PEG M_n~2250 (P-2250) was more effective than Brij and PE-*b*-PEG M_n~1400 (P-1400) to stabilize C16 nano-emulsions through multiple thermal cycles and long-term storage.

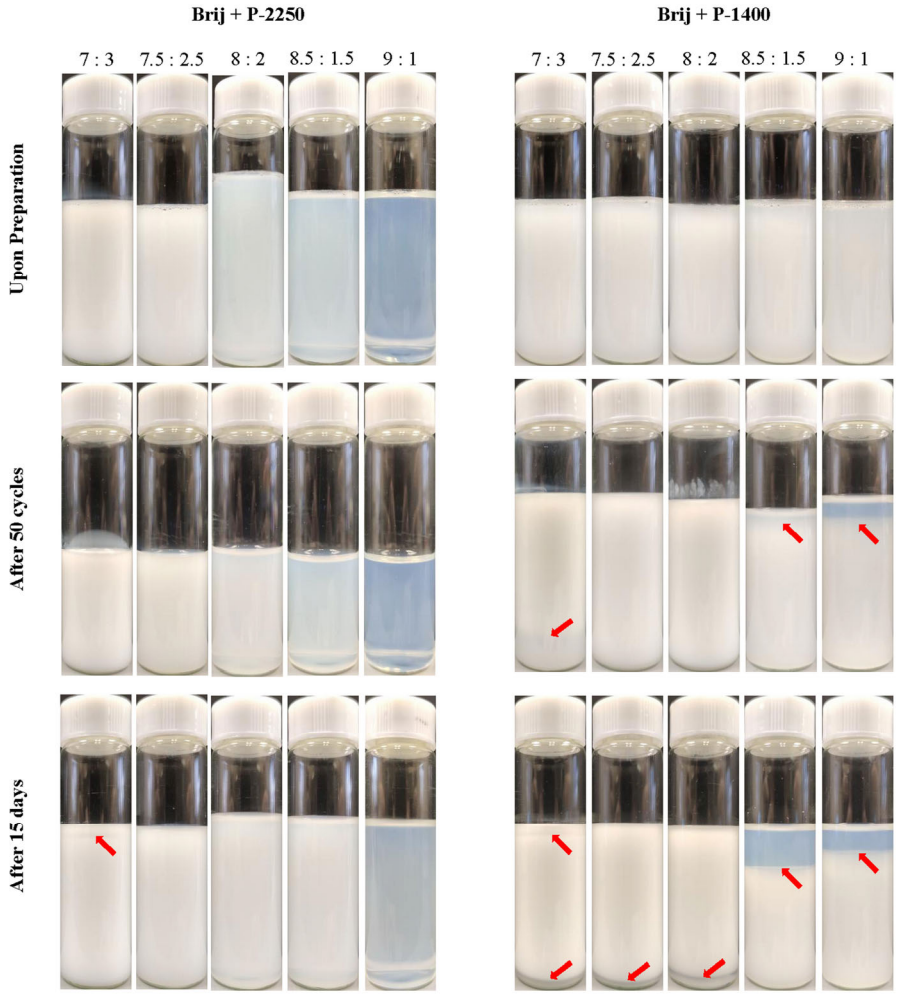

Fig. 1 Photos of 20% n-hexadecane nano-emulsions with 10% surfactant mixtures of Brij and PE-*b*-PEG M_n~2250 (P-2250) or PE-*b*-PEG M_n~1400 (P-1400) at mass ratios from 7:3 to 9:1 upon preparation and after 50 thermal cycles, and 15-day storage at 25 ℃ (red arrows pointing at the break down spots).

Fig. 2 shows the characteristics of nano-emulsions prepared with 20% n-hexadecane and 10% surfactant mixture of Brij and P-2250 at mass ratios from 7:3 to 9:1. As shown in Fig. 2a, the droplet size of nano-emulsions upon preparation decreased with the increase in the mass ratio of Brij to P-2250, from the largest of 122.3 nm (PDI ~0.364) at 7:3 mass ratio to the smallest of 54.4 nm (PDI ~0.163) at 9:1 mass ratio. After 50 thermal cycles, the droplet size of nano-emulsion at 7:3 mass ratio was increased to 135.5 nm, while the other emulsion samples had only a slight change. A notable droplet size increase was also found for the emulsion sample at 8.5:1.5 mass ratio after 15 days. The nano-emulsions exhibited Newtonian fluid behavior because of stable apparent viscosities as the increasing shear rate (Supplementary data,

Fig. S1a). As shown in Fig. 2b, the apparent viscosity increased with the increasing P-2250 content, from 15.7 mPa·s at 1% to a maximum 47.5 mPa·s at 3%, indicating a linear correlation and the significant impact of polymeric surfactant P-2250.

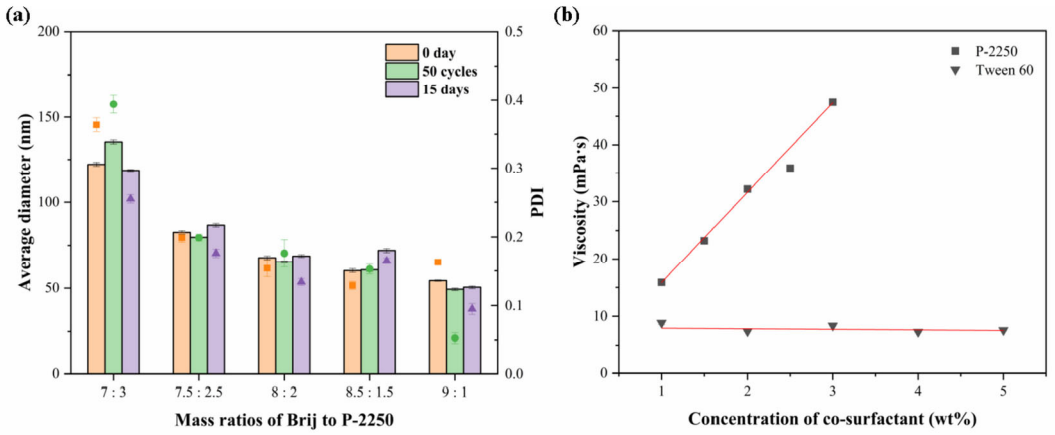

Fig. 2 Characteristics of nano-emulsions containing 20% n-hexadecane and 10% surfactant mixtures of Brij and PE-*b*-PEG M_n~2250 (P-2250) at various mass ratios: (a) droplet size (columns) and PDI (scatter points); (b) apparent viscosity (at 60 s^{-1} and 25 °C) as a function of the co-surfactant (P-2250 or Tween 60) content.

The difference in the emulsion stability with PE-*b*-PEG M_n~1400 and ~2250 (P-1400 and P-2250) was due probably to their difference in the molecular structure, as given in Scheme 1. Both Brij and PE-*b*-PEG can be defined as C_iE_j, where C and E stand for the carbon number of alkyl tail and the ethoxy group number of PEO head, respectively [50]. Specifically, P-2250 ($C_{30}E_{40}$) has a much bigger hydrophilic head group than P-1400 ($C_{48}E_{16}$) providing a stronger steric repulsion to protect the droplets from coalescence. Unlike Brij ($C_{12}E_4$), neither P-2250 nor P-1400 could induce phase inversion and effectively stabilize emulsion alone. Therefore, the emulsion PIT point was mainly determined by the Brij content. On the other hand, P-2250 could notably increase the viscosity of nano-emulsions, contributing positively to the emulsion stability and to the content reduction of Brij. As shown previously [16], a lower Brij content resulted in a higher PIT point, so that the addition of P-2250 could indirectly improve the PIT point and the emulsion stability.

Based on the results, 8:2 mass ratio of Brij to P-2250 was chosen and further explained as follows. Firstly, the Brij and P-2250 mixture afforded more stable C16 nano-emulsions than the Brij and P-1400 combination. Secondly, the nano-emulsion sample at 8:2 mass ratio had a smaller droplet size and a smaller droplet size change after 15-day storage at 25 °C than the samples prepared at 7.5:2.5 or 8.5:1.5 mass ratio. Thirdly, the PIT point of the sample at 8:2

mass ratio was further away from room temperature than that of the sample at 9:1 mass ratio, and the higher viscosity at 8:2 mass ratio may increase the stability of nano-emulsions.

3.1.2. Brij and Tween combinations

Fig. 3 shows the photos of nano-emulsions prepared with mixtures of Brij and Tween 80 or 60 upon preparation and after 50 thermal cycles, and 15 days. Initially, the nano-emulsions displayed bluish and translucent or transparent appearance except for the emulsion sample at 5:5 Brij to Tween 80 mass ratio. However, the nano-emulsions turned milky after 50 thermal cycles and were eventually broken down after 15 days at 8:2 mass ratio of Brij to Tween 80 or 60. The nano-emulsion prepared at 9:1 Brij to Tween 80 mass ratio also exhibited a slight breakdown after 15 days with a condensed milky layer appearing at the top.

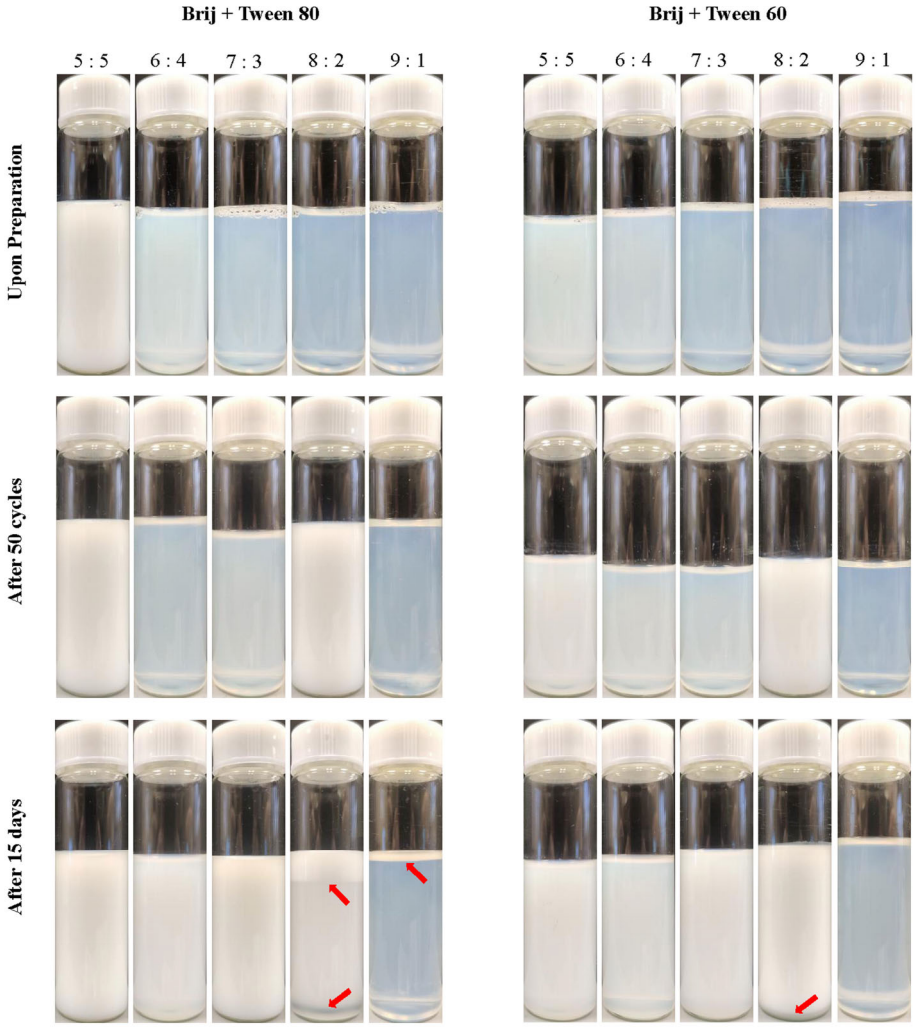

Fig. 3 Photos of 20% n-hexadecane nano-emulsions with 10% surfactant mixtures of Brij and Tween 80 or 60 at mass ratios from 5:5 to 9:1 upon preparation and after 50 thermal cycles, and 15-day storage at 25 °C (red arrows pointing at the break down spots).

Fig. 4 shows the characteristics of nano-emulsions prepared with 20% n-hexadecane and 10% surfactant mixtures of Brij and Tween 80 or 60 from 5:5 to 9:1 mass ratio. As shown in Fig. 4a, a very small droplet size about 50 nm was attained at all Brij to Tween 80 mass ratios except 5:5, and the PDI was less than 0.2 in the initial nano-emulsions. The initial droplet size at 5:5 Brij to Tween 80 mass ratio was 111.3 nm, and was increased to 134.2 nm after 50 thermal cycles. The droplet size at 7:3 Brij to Tween 80 mass ratio was also increased from the 53.7 nm initially to 123 nm after 15 days. Because of emulsion breakdown, the droplet size at 8:2 Brij to Tween 80 mass ratio showed a dramatic increase after 50 thermal cycles or 15-day storage. Additionally, a thin creaming layer on the top of the emulsion sample at 9:1 Brij to Tween 80 mass ratio after 15 days. Although the droplet size was small, a large PDI of ~0.5 could still indicate the high inhomogeneity of the nano-emulsion.

Fig. 4b shows the droplet size and PDI of nano-emulsions prepared by the mixture of Brij and Tween 60. The initial droplet size at 5:5 Brij and Tween 60 mass ratio was 68.9 nm, which was much smaller than that prepared with the same mass ratio of Brij and Tween 80. After 50 thermal cycles and 15-day storage, the three emulsion samples at 5:5, 6:4 and 9:1 mass ratio showed a high stability with only minor changes in the droplet size. Only the nano-emulsion prepared with Brij and Tween 60 at 8:2 mass ratio showed a dramatic increase in the droplet size for a slight emulsion breakdown with a thin aqueous phase present at the bottom after 15 days of storage. Overall, this set of results suggests that Tween 60 was more favourable than Tween 80 to combine with Brij to stabilize the C16 nano-emulsions.

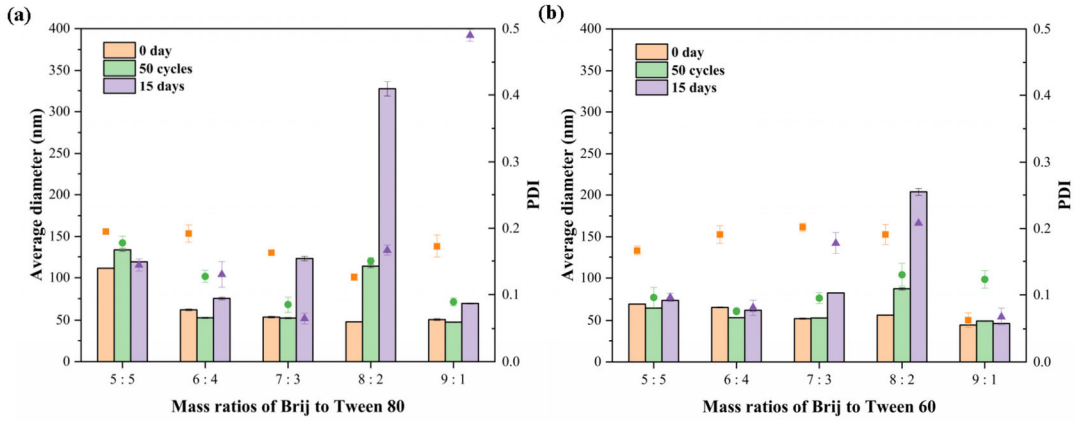

Fig. 4 Characteristics of nano-emulsions containing 20% n-hexadecane and 10% surfactant mixtures of Brij and Tween 80 or 60 at various mass ratio: (a) droplet size (columns) and PDI (scatter points) of nano-emulsions prepared with Brij and Tween 80; (b) droplet size (columns) and PDI (scatter points) of nano-emulsions prepared with Brij and Tween 60.

The nano-emulsions prepared with Brij and Tween 60 exhibited a nearly Newtonian fluid behavior with relatively constant apparent viscosities, all below 10 mPa·s (Supplemental data, Fig. S1b). Unlike polymeric surfactant P-2250, Tween 60 had little effect on the viscosity (Fig. 2b), but a strong influence on the PIT point (derived from Supplemental data Fig. S2), as shown in Table 2. The increasing mass ratio of Tween 60 resulted in a significant increase in the PIT, from about 30 ℃ at 9:1 to over 60 ℃ at 5:5 mass ratio. A main reason is that Tween 60 has a larger PEO head group than Brij (20 vs. 4 ethoxy group number), while a less different alkyl tail group (18 vs. 12 carbon number). The packing parameter of the surfactant layer is lowered with more Tween 60 incorporated into the interface. With this, the nano-emulsions need to be heated to a higher temperature before the PIT point is attained [51].

The nano-emulsion with Brij and Tween 60 at 8:2 mass ratio had a PIT around 36 ℃, which was not much higher than room temperature. As afore mentioned, the interfacial tension would be low and unable to stabilize the droplets against coalescence. In fact, the sample at 8:2 Brij to Tween 60 mass ratio became milky after a few hours at 25 ℃, while it remained bluish transparent after storage at 15 ℃ for about 5 days, indicating that the storage temperature should be around 20-30 ℃ below the PIT point. On the other hand, the nano-emulsion at 9:1 Brij to Tween 60 mass ratio with the lowest PIT point remained stable during the test period. Therefore, the emulsion stability is a highly complicated problem and related to multiple factors.

Based on the above results, the combination of Brij and Tween 60 at the optimal mass ratio of 6:4 was chosen for the following experiments. The PIT point of the sample at 9:1 mass ratio was very low, which would be undesirable for the TES system being constructed for cooling the room that may have a higher ambient temperature. As for the sample at 5:5 mass ratio, it had a larger droplet size and a higher PIT point which would require more energy for fabrication and regeneration of nano-emulsions. Overall, the sample at 6:4 mass ratio was most favourable with a suitable PIT point around 53 ℃, and a smaller droplet size of 61.5 nm after 15-day storage.

3.2. Surfactant content on emulsion properties

Fig. 5 shows the characteristics of 20% nano-emulsions prepared with 8-12% surfactant mixture of Brij and PE-*b*-PEG M_n~2250 (P-2250) at 8:2 mass ratio. As shown in Fig. 5a, the droplet size decreased steadily with increasing surfactant content, approaching a low of 53.0 nm with 12% of the surfactant mixture. As shown in Fig. 5b, the droplet size distribution shifted

to the right with decreasing surfactant content, to droplet size 87.0 nm at 8% surfactant. All nano-emulsion samples showed a high stability with negligible change in the droplet size or size distribution after 50 thermal cycles or 15 days at 25 ℃ (Fig. 5c-Fig. 5g). Similarly, the apparent viscosity of nano-emulsions did not vary significantly with the shear rate, indicative of Newtonian fluid behaviour (Supplemental data, Fig. S1c).

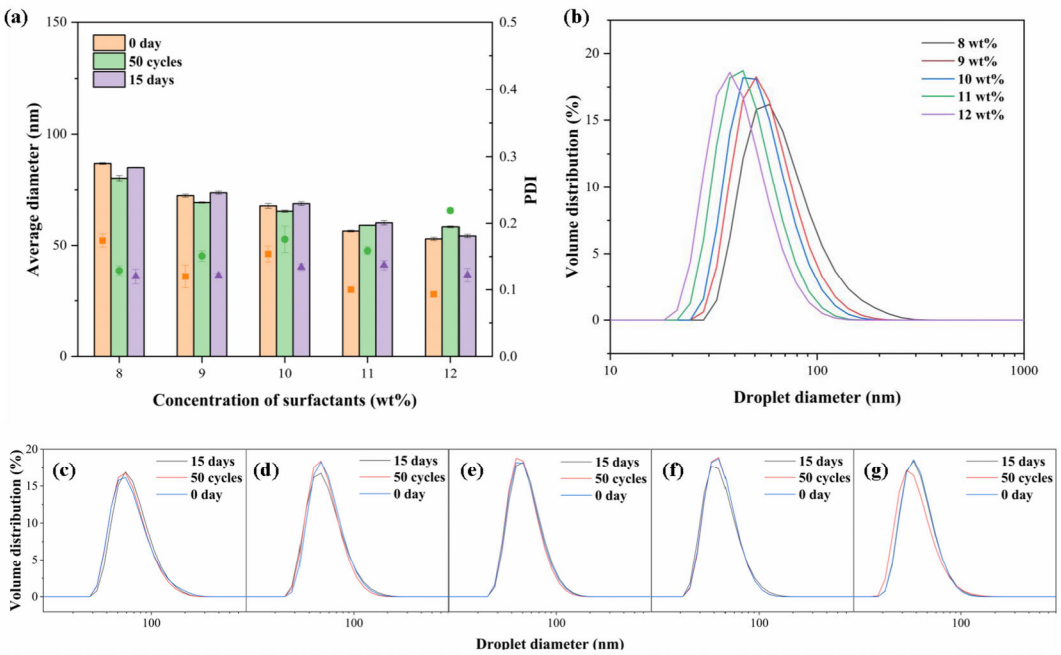

Fig. 5 Characteristics of nano-emulsions containing 20% n-hexadecane and 8-12% surfactant mixture of Brij and P-2250 at 8:2 mass ratio: (a) droplet size (columns) and PDI (scatter points); (b) droplet size distribution upon preparation; (c-g) droplet size distributions of the samples at 8% (c) - 12% (g) of surfactant upon preparation and after 50 thermal cycles, and 15-day storage.

As shown in Fig. 6, the apparent viscosity increased rapidly with the surfactant content, from 11.1 mPa·s at 8% surfactant to 90.5 mPa·s at 12% surfactant, indicating a non-linear relationship with the surfactant content. Based all the results, the final surfactant content was chosen at 11% for the relatively small droplet size, relatively low viscosity and other desirable properties. With 20% PCM and 11% of the surfactant, the corresponding mass ratio PCM to surfactant was 20:11.

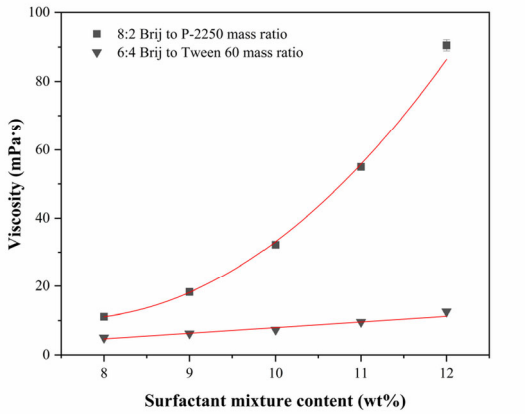

Fig. 6 Apparent viscosity (at 60 s^{-1} shear rate and 25 ℃) as a function of the content of surfactant mixtures (8:2 Brij to P-2250 or 6:4 Brij to Tween 60 mass ratios).

Fig. 7 shows the characteristics of 20% nano-emulsions prepared with 8-12% surfactant mixture of Brij and Tween 60 at 6:4 mass ratio. The droplet size decreased with an increase in the surfactant content, i.e. from 92.5 nm at 8% to 45.6 nm at 12% of surfactant (Fig. 7a), and the size distribution also became smaller and narrower (Fig. 7b). Fig. 7c-Fig. 7g present the droplet size distribution of each emulsion sample with 8-12% surfactant upon preparation and after 50 thermal cycles, and storage for 15 days. A general trend with most of the samples was the shifting of droplet distribution peak to the right after 50 thermal cycles and 15 days. Notice that the droplet size was calculated based on the distribution peak and PDI. A small peak and a high PDI may contribute to a larger droplet size than a large peak and a small PDI, as was the case for the nano-emulsion with 8% surfactant (Fig. 7c). The droplet size distribution upon preparation (blue curve) was 'fat' with a smaller distribution peak at 73.53 nm and a higher PDI of 0.174, while it became 'slimmer' after 15 days (black curve) with a larger peak at 80.07 nm and a smaller PDI of 0.081. This explanation is also valid for most of the nano-emulsions with smaller droplet size after 50 thermal cycles and 15 days.

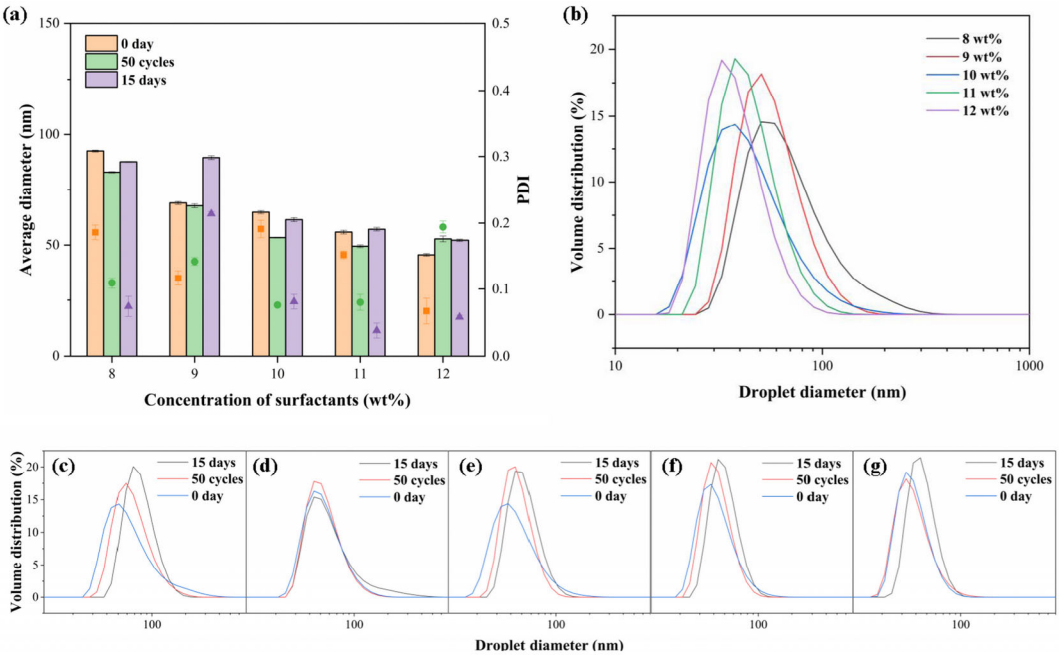

Fig. 7 Characteristics of nano-emulsions containing 20% n-hexadecane and 8-12% surfactant mixture of Brij and Tween 60 at 6:4 mass ratio: (a) droplet size (columns) and PDI (scatter points); (b) droplet size distribution upon preparation; (c-g) droplet size distributions of the samples at 8% (c) - 12% (g) of surfactant upon preparation and after 50 thermal cycles, and 15-day storage.

Table 2 shows the PIT point nano-emulsions as a function of the mass ratio and total content of surfactant mixture, Brij and Tween 60. An increase in the surfactant content resulted in a lower PIT point range but a higher apparent viscosity that was linear with the content of surfactant mixture (Fig. 6). The emulsion sample with 8% of Brij and Tween 60 had the highest PIT range of 56-59 °C and was decreased to 48-51 °C with 12% of the surfactant mixture. The final surfactant content was chosen at 11% for the favourable properties such as the droplet size, apparent viscosity and PIT point. Correspondingly, the mass ratio of the PCM to surfactant mixture of Brij and Tween 60 was 20:11.

Table 2 Variation of the PIT point of nano-emulsions with the mass ratio and content of surfactant mixture Brij and Tween 60.

Brij to Tween 60 mass ratio [a]	PIT point (°C)	Surfactant content [b]	PIT point (°C)
9:1	28-31	8	56-59
8:2	34-38	9	53-56
7:3	41-45	10	51-55
6:4	51-55	11	50-53
5:5	62-65	12	48-51

a. total surfactant content fixed at 10 wt%; b. mass ration of Brij to Tween 60 fixed at 6:4

3.3. Effects of PCM content

A relatively high PCM content is desirable for achieving a high thermal storage density. Considering different effects of the surfactant content on the apparent viscosity, the PCM content at 25% was tested for Brij and P-2250, while a higher PCM content up to 30% was chosen for Brij and Tween 60. The 25% C16 nano-emulsion with 13.75% surfactant mixture of Brij and P-2250 at 8:2 mass ratio formed a gel (Supplemental data, Fig. S3a) as expected from the non-linear relationship of the apparent viscosity to the surfactant content.

The PCM content also had a significant effect on the apparent viscosity, especially with the relatively small droplets [11]. The 25% C16 nano-emulsion with the surfactant mixture of Brij and Tween 60 at 6:4 mass ratio had an apparent viscosity about 52.0 mPa·s, while 30% C16 nano-emulsion was far too viscous, as shown in Fig. S3b, for pipeline transportation. It should be noted that emulsion stability is of a higher priority for consideration as emulsion breakdown can cause drastic reduction of the efficiency or complete failure of the system due to pipeline blockage. Moreover, the working volumetric flow rate in the potential TES system is quite small, so that the pressure drop and pumping power consumption will not be too different from those with water. Consequently, a proper viscosity around 50 mPa·s is desirable for the emulsion stability as well as fluid transportation in pipes. With all these in consideration, the PCM content was recommended as 20% for Brij and P-2250 at 8:2 mass ratio or 25% for Brij and Tween 60 at 6:4 mass ratio, respectively.

3.4. Thermal properties

To reduce the high supercooling of n-hexadecane (C16) nano-emulsions, n-alkane n-

octacosane (C28) was added as a nucleating agent. As shown in Table 3, the bulk C16 had a latent heat of ~245 J/g and supercooling degree of 1.25 ℃. Without the addition of nucleating agents, the supercooling degree of 20% C16 nano-emulsion stabilized by Brij and PE-*b*-PEG M_n~2250 (P-2250) was 5.13 ℃, and the latent heat was about 41 J/g, which was lower than the theoretical value of 49 J/g. The latent heat decrease of alkanes after emulsification is quite common as reported previously [52-54], which is mainly attributed to the difference of crystal morphology in bulk and in nano-droplet. For instance, Montenegro and Landfester [55] have shown the difference in the XRD intensities of bulk n-hexadecane and n-hexadecane nano-emulsions, indicating the change in the crystal morphology. In addition, the latent heats of 20% and 25% n-hexadecane nano-emulsions were in the range of ~40 J/g to ~50 J/g (Table 3). The onset melting temperature was also decreased to 11.57 ℃. The difference between the bulk and the droplet melting point (ΔT_m) is governed by the Gibbs-Thomson equation [56]:

$$\Delta T_m = \frac{2T_m \gamma_{sl} v_l}{\Delta_{sl} H} \tag{5}$$

where T_m is the melting point of bulk liquid, γ_{sl} is the interfacial tension, v_l is the molar volume of the liquid, and $\Delta_{sl}H$ is the molar enthalpy of melting. With the addition of C28, the onset freezing point was gradually increased while the onset melting temperature remained at a similar value. The supercooling degree was reduced to 3.77 ℃ at 2% C28 concentration , but the latent heat experienced a slight drop to 39 J/g.

Table 3 Melting and freezing properties of C16 nano-emulsions with C28 as a nucleating agent.

Content (wt%)	ΔH_m (J/g)	ΔH_f (J/g)	Onset T_m (℃)	Onset T_f (℃)	ΔT (℃)
20% C16 nano-emulsions with 11% Brij and P-2250 at 8:2 mass ratio					
Bulk C_{16}	-244.75	247.94	17.40	16.15	1.25
0	-41.31	41.09	11.57	6.44	5.13
0.5	-39.63	39.99	11.84	7.70	4.14
1.0	-37.67	37.62	11.97	7.80	4.17
1.5	-38.40	38.75	12.03	8.08	3.95
2.0	-39.09	39.43	12.11	8.34	3.77
25% C16 nano-emulsions with 13.75% Brij and Tween 60 at 6:4 mass ratio					
0	-47.55	48.05	12.51	3.47	9.04

0.5	-51.11	51.49	12.24	4.05	8.19
1.0	-48.34	48.47	12.25	5.05	7.20
1.5	-49.76	50.20	12.13	6.31	5.82
2.0	-49.51	49.87	12.49	1^{st}: 7.71 2^{nd}: 5.13	4.78
2.5	-50.88	51.81	12.44	1^{st}: 10.03 2^{nd}: 5.20	2.41

Table 3 also shows the thermal properties of 25% C16 nano-emulsions stabilized with Brij and Tween 60. Without the addition of C28, the supercooling degree was 9.04 ℃, which was consistent with the previously reported value of 8.93 ℃ using single Brij as surfactant [16], indicating that Tween 60 had no effect on the supercooling reduction. On the other hand, it was much higher than the corresponding value of 5.13 ℃ when the mixture of Brij and P-2250 was used, implying that P-2250 was effective to reduce the supercooling. Moreover, a few emulsion samples formed with Brij and PE-*b*-PEG M_n~1400 (P-1400) were also analysed by DSC upon preparation, though the data was not shown because of their poor stability. On the other hand, the supercooling degrees of the nano-emulsions with Brij to P-1400 mass ratio were up to 7.0 ℃, much higher than the emulsions prepared with Brij and P-2500. Compared with P2500 ($C_{30}E_{40}$), P-1400 ($C_{48}E_{16}$) with a longer hydrocarbon chain was less effective to lower the supercooling. This result suggests that structure characteristics other than the chain length of hydrocarbon molecules are also important factors affecting the nucleation of nano-emulsions.

Similarly, the addition of C28 had little effect on the onset melting point but increased the onset freezing point. As a result, the lowest supercooling degree was 2.41 ℃ at 2.5% C28 content. However, two separated freezing peaks were observed with the second peak at 5.2 ℃. The second peak started to appear at 2% C28 content and remained still with the onset freezing point at around 5 ℃, which was close to that at 1% C28. The presence of double freezing points was probably attributed to the formation of different crystal forms of C16 in nano droplets at a high C28 content. Based on this set of experiments, 2% was chosen as the optimal content due to the low supercooling degree and mainly singular crystallization curves (Supplemental data, Fig. S4).

3.5. Stability after repeated thermal cycles and long period storage

The two PCM nano-emulsions from above were further evaluated for long-term stability after 300 thermal cycles and long period of storage. Fig. 8 displays the characteristics of nano-emulsion with 20% C16, 11% the Brij and P-2250 mixture and 2% C28, designated A. As

shown in Fig. 8a, the initial nano-emulsion A had a narrow size distribution and a small droplet size of 68.94 nm (Table 4). However, there was 1.1% volume of the C16 droplets at the distribution peak of 4-6 μm. This may be attributed to the high viscosity of coarse W/O emulsion when crossing the PIT zone, which may affect the interfacial arrangement of P-2250. Nano-emulsion A was very stable with small droplet size change after 30 days and 300 thermal cycles, while the volume proportion at the distribution peak of 4-6 μm further increased to 1.5% and 1.8%, respectively. For a longer storage period up to 90 days, the lower layer had 1.8% volume at the distribution peak of 4-6 μm, which resulted in an increasing droplet size to 80.89 nm. Correspondingly, the upper layer had no distribution peak at 4-6 μm and therefore a smaller droplet size of 67.83 nm.

Fig. 8b shows the DSC curves of nano-emulsion A upon preparation and after 300 thermal cycles and long period storage. Thermal properties were changed, such as an increase in the supercooling degree to 6.63 ℃ and a slight decrease of latent heat after 300 thermal cycles, or little change in the supercooling degree but a notable decrease of latent heat to about 37.5 J/g after 30 days. Besides, the upper layer of nano-emulsion A after 90 days had better thermal properties, e.g., higher latent heat and lower supercooling degree, than the lower layer. As shown in Fig. 8c, the photos of nano-emulsion A are more obvious to explain the change. The initial nano-emulsion A showed an optical translucent appearance, but turned milky with a larger droplet size and higher supercooling degree after 300 thermal cycles. After storage for 30 days, the appearance of nano-emulsion A was still similar to the initial, suggesting little change in the droplet size and supercooling degree. For a longer period (90 days), the lower layer of nano-emulsion A became milky but no obvious change in the upper layer, implying differences in the nano-emulsion properties. Moreover, although C28 had good compatibility with C16, the addition of C28 may induce the emulsion instability since 20% C16 nano-emulsion with no C28 remained uniform and translucent for over 120 days. Fig. 8d gives the micrograph of initial nano-emulsion A under the optical microscope, where only very small and uniform PCM droplets were observed.

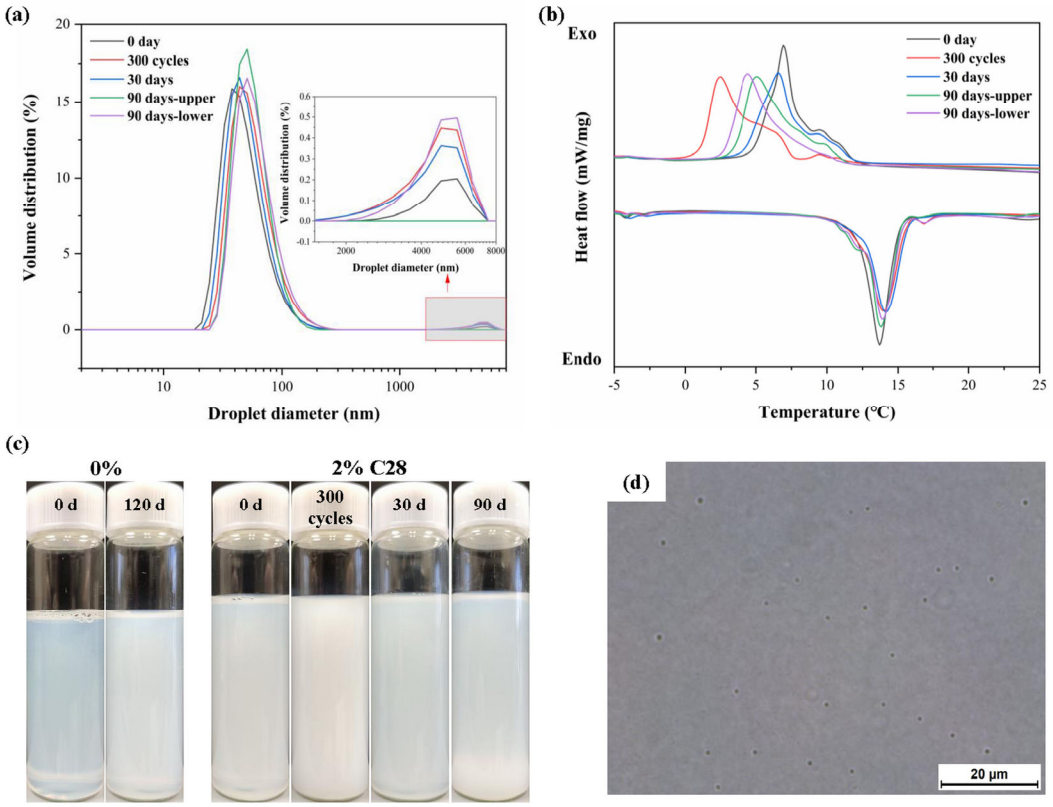

Fig. 8 Characteristics of nano-emulsion A with 20% n-hexadecane, 11% the mixture of Brij and P-2250 at 8:2 mass ratio and 2% C28 as a nucleating agent: (a) the droplet size distribution; (b) DSC curves; (c) photos of nano-emulsion A, and the corresponding sample without C28; (d) micrograph under optical microscope (1000×).

Table 4 The droplet size and thermal properties of nano-emulsion A and B.

	Stage	Diameter (nm)	PDI	ΔH_m (J/g)	ΔH_f (J/g)	ΔT (°C)
A	0 day	68.94 ± 0.15	0.202 ± 0.005	-39.09	39.43	3.77
	300 cycles	79.88 ± 0.74	0.229 ± 0.002	-38.66	38.50	6.63
	30 days	72.82 ± 0.84	0.233 ± 0.010	-37.31	37.56	4.08
	90 days-upper	67.83 ± 0.21	0.114 ± 0.005	-38.98	39.83	4.63
	90 days-lower	80.89 ± 0.29	0.206 ± 0.009	-34.81	35.16	5.47
B	0 day	57.20 ± 0.98	0.085 ± 0.010	-49.51	49.87	4.78
	300 cycles	56.29 ± 0.35	0.210 ± 0.011	-49.51	50.54	5.04
	120 days	70.72 ± 1.05	0.063 ± 0.008	-50.03	50.71	5.00

564 The above results of nano-emulsion A suggest that polymeric surfactant detachment may
565 occur after multiple thermal cycles or long period storage. It would be difficult for P-2250 to
566 be reabsorbed at the interface due probably to its big molecular weight, leading to a higher
567 supercooling degree after 300 thermal cycles. Meanwhile, the detached P-2250 would sediment
568 after long period leading to the differences of the droplet size and thermal properties between
569 the upper and lower layers.
570 Fig. 9 shows the characteristics of nano-emulsion with 25% C16, 13.75% the Brij and
571 Tween 60 mixture and 2% C28, designated B. As shown in Fig. 9a, the initial size distribution
572 of nano-emulsion B was narrow with small droplet size of 57.20 nm, which had a small shift
573 to the right after 120 days storage with the increasing droplet size 70.72 nm. After 300 thermal
574 cycles, a small portion (1% by volume) of the C16 droplets at the distribution peak of 4-6 μm
575 appeared with the main distribution peak staying still. Unlike nano-emulsion A, nano-emulsion
576 B was more stable in terms of thermal properties as very small differences between the
577 supercooling degree and latent heat after 120 days and 300 thermal cycles (Fig. 9b). As seen
578 from the photos in Fig. 9c, the initial nano-emulsion B exhibited a bluish transparent color and
579 became optical translucent after 300 thermal cycles and 90 days storage. The main reason could
580 be either a small volume proportion at the distribution peak of 4-6 μm or a shifting main
581 distribution peak. On the other hand, the addition of C28 seemed to have the positive effect on
582 the emulsion stability, comparing to the appearances of nano-emulsions with and without C28
583 after 120 days. It further illustrates that the mechanism of emulsion instability is complicated
584 and the same factor may have different effect depending on the different oil/surfactant systems.
585 The micrograph of initial nano-emulsion B was given in Fig. 9d, where it contained very small
586 and uniform PCM droplets, consisting with the droplet size detected by the DLS. Overall, nano-
587 emulsion B had the better stability and more stable thermal properties than nano-emulsion A,
588 which showed great potential for further development and application as a cool storage medium
589 for the TES systems.
590

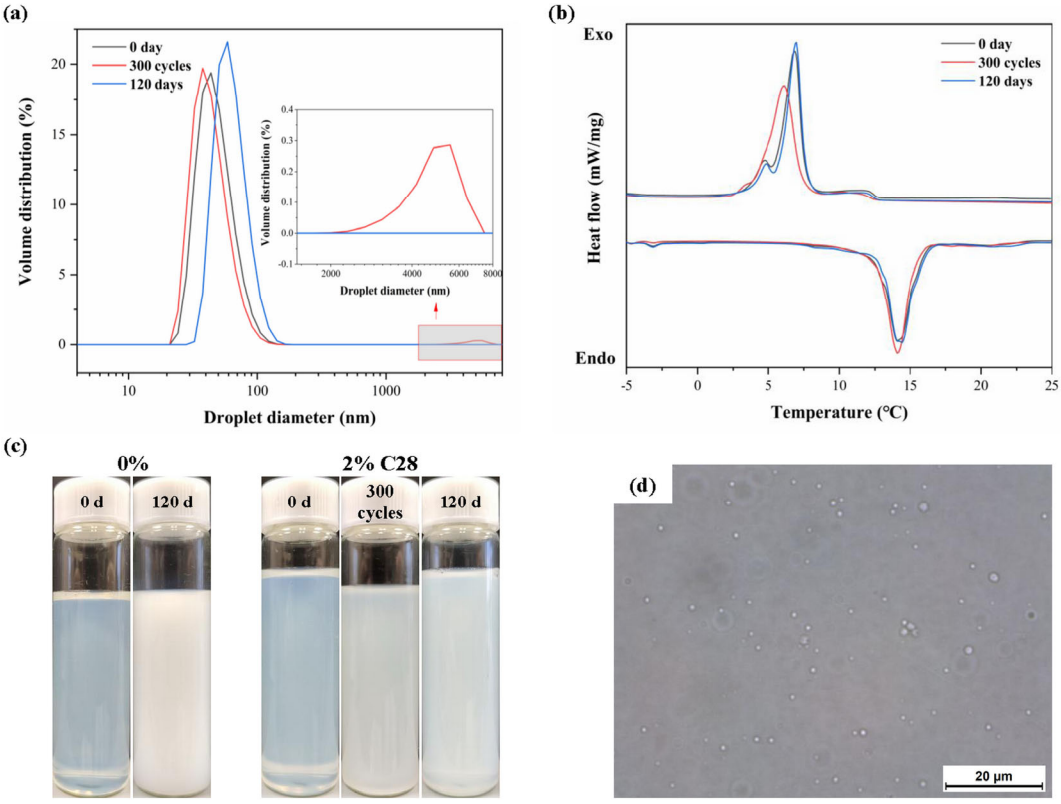

Fig. 9 Characteristics of nano-emulsion B with 25% n-hexadecane, 13.75% the Brij and Tween 60 mixture at 6:4 mass ratio and 2% C28 as a nucleating agent: (a) the droplet size distribution; (b) DSC curves; (c) photos of nano-emulsion B, and the corresponding sample without C28; (d) micrograph under optical microscope (1000×).

4. Conclusions

Highly stable n-hexadecane PCM nano-emulsions have been fabricated through the use of two surfactants in combination, Brij L4 as the primary and PE-*b*-PEG M_n~2250 (P-2250) or Tween 60 as the co-surfactant. The droplet size of nano-emulsions was well controlled within 100 nm, which was mainly dependent upon the content of primary surfactant, while the polymeric co-surfactant P-2250 had a significant influence on the viscosity and a positive effect to lowering the supercooling degree, due probably to its long hydrocarbon chain promoting the nucleation of n-hexadecane in nano-droplets. The hydrophilic surfactant Tween 60 was effective to raise the PIT point to above 50 ℃, though it had little effect on the supercooling of nano-emulsions. In addition to the type and combination of surfactants, the mass ratios of two surfactants in the mixture and the relative content of surfactant to PCM were major factors for the formulation of stable nano-emulsions. After systematic evaluation of these factors, a few optimized formations of n-hexadecane nano-emulsions were derived, exhibiting a

Newtonian-flow behaviour with a low viscosity of ~50 mPa·s and a low supercooling degree of 3-4 ℃, which could sustain multiple thermal cycles and long period of storage. Further study is undergoing to test the optimized PCM nano-emulsions in a pilot TES system and to evaluate their dynamic stability and performance. Moreover, more effective measures need to be developed to achieve and maintain a much lower degree of supercooling of the PCM nano-emulsions.

Acknowledgments

This work was supported financially by the Environment and Conservation Fund (ECF Project 53/2018), the Research Grant Council of the Hong Kong SAR Government through General Research Fund (PolyU 152707/16E), and by the Hong Kong Polytechnic University.

References

[1] A. Sharma, V.V. Tyagi, C.R. Chen, D. Buddhi, Review on thermal energy storage with phase change materials and applications, Renewable and Sustainable Energy Reviews, 13 (2009) 318-345.

[2] G. Alva, Y. Lin, G. Fang, An overview of thermal energy storage systems, Energy, 144 (2018) 341-378.

[3] N.H.S. Tay, M. Liu, M. Belusko, F. Bruno, Review on transportable phase change material in thermal energy storage systems, Renewable and Sustainable Energy Reviews, 75 (2017) 264-277.

[4] D. Zhou, C.Y. Zhao, Y. Tian, Review on thermal energy storage with phase change materials (PCMs) in building applications, Applied Energy, 92 (2012) 593-605.

[5] L.F. Cabeza, A. Castell, C. Barreneche, A. de Gracia, A.I. Fernández, Materials used as PCM in thermal energy storage in buildings: A review, Renewable and Sustainable Energy Reviews, 15 (2011) 1675-1695.

[6] H. Nazir, M. Batool, F.J. Bolivar Osorio, M. Isaza-Ruiz, X. Xu, K. Vignarooban, P. Phelan, Inamuddin, A.M. Kannan, Recent developments in phase change materials for energy storage applications: A review, International Journal of Heat and Mass Transfer, 129 (2019) 491-523.

[7] Y. Wang, Z. Chen, X. Ling, An experimental study of the latent functionally thermal fluid with micro-encapsulated phase change material particles flowing in microchannels, Applied Thermal Engineering, 105 (2016) 209-216.

[8] C. Liu, Z. Ma, J. Wang, Y. Li, Z. Rao, Experimental research on flow and heat transfer characteristics of latent functional thermal fluid with microencapsulated phase change materials, International Journal of Heat and Mass Transfer, 115 (2017) 737-742.
[9] D. Cabaleiro, F. Agresti, S. Barison, M.A. Marcos, J.I. Prado, S. Rossi, S. Bobbo, L. Fedele, Development of paraffinic phase change material nanoemulsions for thermal energy storage and transport in low-temperature applications, Applied Thermal Engineering, 159 (2019) 113868.
[10] Z. Ding, H. Zhang, F. He, Y. Li, R. He, K. Zhang, J. Fan, Z. Yang, W. Yang, Novel paraffin/ethylene propylene diene monomer phase change latex with excellent stability and low viscosity, Solar Energy Materials and Solar Cells, 200 (2019) 109957.
[11] F. Wang, W. Lin, Z. Ling, X. Fang, A comprehensive review on phase change material emulsions: Fabrication, characteristics, and heat transfer performance, Solar Energy Materials and Solar Cells, 191 (2019) 218-234.
[12] Z. Youssef, A. Delahaye, L. Huang, F. Trinquet, L. Fournaison, C. Pollerberg, C. Doetsch, State of the art on phase change material slurries, Energy Conversion and Management, 65 (2013) 120-132.
[13] J. Shao, J. Darkwa, G. Kokogiannakis, Review of phase change emulsions (PCMEs) and their applications in HVAC systems, Energy and Buildings, 94 (2015) 200-217.
[14] P. Schalbart, M. Kawaji, K. Fumoto, Formation of tetradecane nanoemulsion by low-energy emulsification methods, International Journal of Refrigeration, 33 (2010) 1612-1624.
[15] J. Chen, P. Zhang, Preparation and characterization of nano-sized phase change emulsions as thermal energy storage and transport media, Applied Energy, 190 (2017) 868-879.
[16] X. Zhang, J. Niu, J.-y. Wu, Evaluation and manipulation of the key emulsification factors toward highly stable PCM-water nano-emulsions for thermal energy storage, Solar Energy Materials and Solar Cells, 219 (2021) 110820.
[17] X. Zhang, J. Niu, J.-Y. Wu, Development and characterization of novel and stable silicon nanoparticles-embedded PCM-in-water emulsions for thermal energy storage, Applied Energy, 238 (2019) 1407-1416.
[18] H. Mehling, L.F. Cabeza, Heat and cold storage with PCM, Springer, 2008.
[19] E. Günther, L. Huang, H. Mehling, C. Dötsch, Subcooling in PCM emulsions – Part 2: Interpretation in terms of nucleation theory, Thermochimica Acta, 522 (2011) 199-204.
[20] A. Safari, R. Saidur, F.A. Sulaiman, Y. Xu, J. Dong, A review on supercooling of Phase Change Materials in thermal energy storage systems, Renewable and Sustainable Energy Reviews, 70 (2017) 905-919.

675 [21] M.H. Zahir, S.A. Mohamed, R. Saidur, F.A. Al-Sulaiman, Supercooling of phase-change
676 materials and the techniques used to mitigate the phenomenon, Applied Energy, 240 (2019)
677 793-817.
678 [22] F. Wang, C. Zhang, J. Liu, X. Fang, Z. Zhang, Highly stable graphite nanoparticle-
679 dispersed phase change emulsions with little supercooling and high thermal conductivity for
680 cold energy storage, Applied Energy, 188 (2017) 97-106.
681 [23] N. Xiang, Y. Yuan, L. Sun, X. Cao, J. Zhao, Simultaneous decrease in supercooling and
682 enhancement of thermal conductivity of paraffin emulsion in medium temperature range with
683 graphene as additive, Thermochimica Acta, 664 (2018) 16-25.
684 [24] T. Sakai, Y. Nakagawa, K. Iijima, Hexadecane-in-water emulsions as thermal-energy
685 storage and heat transfer fluids: Connections between phase-transition temperature and period
686 of hexadecane droplets dispersed in hexadecane-in-water emulsions and characteristics of
687 surfactants, Colloids and Surfaces A: Physicochemical and Engineering Aspects, 529 (2017)
688 394-402.
689 [25] D.J. McClements, S.R. Dungan, J.B. German, C. Simoneau, J.E. Kinsella, Droplet Size
690 and Emulsifier Type Affect Crystallization and Melting of Hydrocarbon-in-Water Emulsions,
691 Journal of Food Science, 58 (1993) 1148-1151.
692 [26] K. Golemanov, S. Tcholakova, N.D. Denkov, T. Gurkov, Selection of Surfactants for
693 Stable Paraffin-in-Water Dispersions, undergoing Solid−Liquid Transition of the Dispersed
694 Particles, Langmuir, 22 (2006) 3560-3569.
695 [27] G. Hagelstein, S. Gschwander, Reduction of supercooling in paraffin phase change slurry
696 by polyvinyl alcohol, International Journal of Refrigeration, 84 (2017) 67-75.
697 [28] R. Strey, Phase behavior and interfacial curvature in water-oil-surfactant systems, Current
698 Opinion in Colloid & Interface Science, 1 (1996) 402-410.
699 [29] D.J. McClements, S.M. Jafari, Improving emulsion formation, stability and performance
700 using mixed emulsifiers: A review, Advances in Colloid and Interface Science, 251 (2018) 55-
701 79.
702 [30] A. Perazzo, V. Preziosi, S. Guido, Phase inversion emulsification: Current understanding
703 and applications, Advances in Colloid and Interface Science, 222 (2015) 581-599.
704 [31] N. Anton, P. Gayet, J.-P. Benoit, P. Saulnier, Nano-emulsions and nanocapsules by the
705 PIT method: An investigation on the role of the temperature cycling on the emulsion phase
706 inversion, International Journal of Pharmaceutics, 344 (2007) 44-52.
707 [32] I. Paunovic, A.K. Mehrotra, Liquid–solid phase transformation of C16H34, C28H58 and
708 C41H84 and their binary and ternary mixtures, Thermochimica Acta, 356 (2000) 27-38.

[33] H. Peng, D. Zhang, X. Ling, Y. Li, Y. Wang, Q. Yu, X. She, Y. Li, Y. Ding, n-Alkanes Phase Change Materials and Their Microencapsulation for Thermal Energy Storage: A Critical Review, Energy & Fuels, 32 (2018) 7262-7293.
[34] P. Fernandez, V. André, J. Rieger, A. Kühnle, Nano-emulsion formation by emulsion phase inversion, Colloids and Surfaces A: Physicochemical and Engineering Aspects, 251 (2004) 53-58.
[35] G. Höhne, W.F. Hemminger, H.-J. Flammersheim, Differential scanning calorimetry, Springer Science & Business Media, 2013.
[36] G.R. Deen, J. Skovgaard, J.S. Pedersen, 6 - Formation and properties of nanoemulsions, in: A.M. Grumezescu (Ed.) Emulsions, Academic Press, 2016, pp. 193-226.
[37] W. Jin, W. Xu, H. Liang, Y. Li, S. Liu, B. Li, 1 - Nanoemulsions for food: properties, production, characterization, and applications, in: A.M. Grumezescu (Ed.) Emulsions, Academic Press, 2016, pp. 1-36.
[38] P.C. Hiemenz, R. Rajagopalan, Principles of Colloid and Surface Chemistry, revised and expanded, CRC press, 2016.
[39] D.J. McClements, Nanoemulsions versus microemulsions: terminology, differences, and similarities, Soft Matter, 8 (2012) 1719-1729.
[40] D.J. McClements, Edible nanoemulsions: fabrication, properties, and functional performance, Soft Matter, 7 (2011) 2297-2316.
[41] J. Boyd, C. Parkinson, P. Sherman, Factors affecting emulsion stability, and the HLB concept, Journal of Colloid and Interface Science, 41 (1972) 359-370.
[42] M. Koroleva, T. Nagovitsina, E. Yurtov, Nanoemulsions stabilized by non-ionic surfactants: stability and degradation mechanisms, Physical Chemistry Chemical Physics, 20 (2018) 10369-10377.
[43] E.R. Garrett, Prediction of Stability of Drugs and Pharmaceutical Preparations, Journal of Pharmaceutical Sciences, 51 (1962) 811-833.
[44] A.S. Kabalnov, E.D. Shchukin, Ostwald ripening theory: applications to fluorocarbon emulsion stability, Advances in Colloid and Interface Science, 38 (1992) 69-97.
[45] K. Shinoda, H. Saito, The effect of temperature on the phase equilibria and the types of dispersions of the ternary system composed of water, cyclohexane, and nonionic surfactant, Journal of Colloid and Interface Science, 26 (1968) 70-74.
[46] J.S. Komaiko, D.J. McClements, Formation of Food-Grade Nanoemulsions Using Low-Energy Preparation Methods: A Review of Available Methods, Comprehensive Reviews in Food Science and Food Safety, 15 (2016) 331-352.

[47] A.H. Saberi, Y. Fang, D.J. McClements, Thermal reversibility of vitamin E-enriched emulsion-based delivery systems produced using spontaneous emulsification, Food Chemistry, 185 (2015) 254-260.
[48] J. Rao, D.J. McClements, Stabilization of Phase Inversion Temperature Nanoemulsions by Surfactant Displacement, Journal of Agricultural and Food Chemistry, 58 (2010) 7059-7066.
[49] I. Mira, N. Zambrano, E. Tyrode, L. Márquez, A.A. Peña, A. Pizzino, J.-L. Salager, Emulsion Catastrophic Inversion from Abnormal to Normal Morphology. 2. Effect of the Stirring Intensity on the Dynamic Inversion Frontier, Industrial & Engineering Chemistry Research, 42 (2003) 57-61.
[50] O. Squillace, C. Esnault, J.-F. Pilard, G. Brotons, Grafting Commercial Surfactants (Brij, CiEj) and PEG to Electrodes via Aryldiazonium Salts, ACS Applied Materials & Interfaces, 9 (2017) 42313-42326.
[51] D. Myers, Surfactant science and technology, John Wiley & Sons, 2020.
[52] T. Kawanami, K. Togashi, K. Fumoto, S. Hirano, P. Zhang, K. Shirai, S. Hirasawa, Thermophysical properties and thermal characteristics of phase change emulsion for thermal energy storage media, Energy, 117 (2016) 562-568.
[53] C.J. Ho, K.-H. Lin, S. Rashidi, D. Toghraie, W.-M. Yan, Experimental study on thermophysical properties of water-based nanoemulsion of n-eicosane PCM, Journal of Molecular Liquids, 321 (2021) 114760.
[54] J. Shao, J. Darkwa, G. Kokogiannakis, Development of a novel phase change material emulsion for cooling systems, Renewable Energy, 87 (2016) 509-516.
[55] R. Montenegro, K. Landfester, Metastable and Stable Morphologies during Crystallization of Alkanes in Miniemulsion Droplets, Langmuir, 19 (2003) 5996-6003.
[56] R. Montenegro, M. Antonietti, Y. Mastai, K. Landfester, Crystallization in Miniemulsion Droplets, The Journal of Physical Chemistry B, 107 (2003) 5088-5094.